**Technical Note**

# Eddy-Current Induction in Extended Metallic Parts As a Source of Considerable Torsional Moment

Hansjörg Graf, PhD,* Ulrike A. Lauer, MSc, and Fritz Schick, PhD, MD

**Purpose:** To examine eddy-current-provoked torque on conductive parts due to current induction from movement through the fringe field of the MR scanner and from gradient switching.

**Materials and Methods:** For both cases, torque was calculated for frames of copper, aluminum, and titanium, inclined to 45° to $B_0$ (maximum torque case). Conditions were analyzed in which torque from gravity (legal limit, ASTM F2213-02) was exceeded. Experiments were carried out on a 1.5 T and a 3 T scanner for copper and titanium frames and plates ($\approx 50 \times 50$ mm$^2$). Movement-induced torque was measured at patient table velocity (20 cm/second). Alternating torque from gradient switching was investigated by holding the specimens in different locations in the scanner while executing sequences that exploited the gradient capabilities (40 mT/m).

**Results:** The calculations predicted that movement-induced torque could exceed torque from gravity (depending on the part size, electric resistance, and velocity). Two experiments on moving conductive frames in the fringe fields of the scanners confirmed the calculations. For maximum torque case parameters, gradient-switching-induced torque was calculated to be nearly 100 times greater than the movement-induced torque. Well-conducting metal parts located off center vibrated significantly due to impulse-like fast alternating torque characteristics.

**Conclusion:** Torque on metal parts from movement in the fringe field is weak under standard conditions, but for larger parts the acceptable limit can be reached with a high static field and increased velocity. Vibrations due to gradient switching were confirmed and may explain the sensations occasionally reported by patients with implants.

**Key words:** MR safety; torque; eddy current; implant; instrument
**J. Magn. Reson. Imaging 2006;23:585–590.**


Section on Experimental Radiology, Department of Diagnostic Radiology, University Hospital Tübingen, Tübingen, Germany.

Contract grant sponsor: German Ministry for Education and Research; Contract grant number: 16SV1351; Contract grant sponsor: Deutsche Forschungsgemeinschaft; Contract grant number: TH 812/1-1.

*Address reprint requests to: H.G., Section on Experimental Radiology, University Hospital Tübingen, Hoppe Seyler Str. 3, D-72076 Tübingen, Germany.
E-mail: hansjoerg.graf@med.uni-tuebingen.de

Received December 13, 2005; Accepted December 28, 2005.
DOI 10.1002/jmri.20539
Published online 13 March 2006 in Wiley InterScience (www.interscience.wiley.com).

ONE ASPECT OF MR SAFETY TESTING of medical implants and instruments is determining whether hazardous torque can occur in the electromagnetic environment of an MR scanner. According to the standard ASTM F2213-02 (1), torque is considered to act on implants made of magnetic materials. Deviation from spherical symmetry causes them to align with the static field $B_0$ (2). Dangerous effects from torque are significantly more difficult to estimate compared to accelerating forces in the fringe field region of the scanner. The lever law has to be considered, and furthermore high forces can result near the pivotal point (2). According to the above-mentioned standard, magnetically induced torque has to be smaller than the product of the maximum device length and device weight, i.e., the mechanical torque $T_{me}$ due to gravity. Several medical products as surgical instruments or prosthetic heart valves have been examined for hazardous torque in the MR environment applying at least the limits in this standard (3–12).

In contrast to ASTM F2213-02, the present paper addresses eddy-current-induced torque on medical implants made of electrically conducting materials. A change in the magnetic flux through such a device induces the eddy current and gives the device a magnetic moment. If the geometry of the device demands an eddy-current development resulting in a magnetic moment that is not aligned parallel to $B_0$, torque will occur. Changing magnetic flux through a metallic part can result from the movement of the part in the fringe field of the scanner, or from gradient switching if the part is positioned off center inside the scanner. Conditions for eddy-current-induced torque were investigated for both cases. Similarly to the situation of torque acting on magnetic material, a complex dependence on implant geometry has to be expected. To gain insight into the order of magnitude of possible effects, we examined rectangular wire frames. This simple geometry allowed us to estimate the resulting amount of torque and perform a comparison with the limits given in ASTM F2213-02.

It should be noted that another relevant condition with changing magnetic flux through a metallic part has already been reported and analyzed: rotation of conductive discs, such as mechanical heart valves, lead to interactions between the induced electrical current and the outer magnetic field (13).

## MATERIALS AND METHODS

### *Theory*

The direction of the magnetic moment related to the induced eddy currents depends on the geometry of the metallic part. To investigate eddy-current-induced torque, we modeled the devices as frames from conducting material, with $l_s$ = length of short side, $l_l$ = length of long side, $A$ = area of the frame, and $q$ = cross section of the conductor. Materials with different specific resistance ρ (resistance per unit length times cross-sectional area of conductor [Ω · m]) were taken into account.

The voltage $U_{ind}$ induced by changing magnetic flux ϕ through the frame without rotation of the frame (constant effective area) obeys Faraday's law:

$$U_{ind} = \frac{d\Phi}{dt} = \frac{d(\vec{A}\cdot\vec{B})}{dt} = \vec{A}\cdot\frac{d\vec{B}}{dt} = A\cdot\frac{dB}{dt}. \quad (1)$$

where $B$ is the magnetic field at a certain location, and $dB/dt$ is its change with time. The electric DC resistance $R$ of the frame can be calculated from

$$R = \rho\cdot\frac{2(l_s + l_l)}{q} \quad (2)$$

The resulting eddy current $I_{eddy}$ is given by

$$I_{eddy} = \frac{U_{ind}}{R} \quad (3)$$

In general, the flux change through the frame resulting from all components of $B$ has to be regarded. If the change of the z-component dominates, torque $T_{el}$ for an inclination θ between the normal of the frame area and the direction of $B$ (Fig. 1) is obtained from

$$T_{el} = 2(F_L\cdot l_l\cdot\sin(\theta)/2) = B\cdot I_{eddy}\cdot l_s\cdot l_l\cdot\sin(\theta) = B\cdot\frac{dB}{dt}\cdot\frac{A^2}{R}\cdot\cos(\theta)\sin(\theta) \quad (4)$$

where $F_L$ denotes the Lorentzian force on the short side of the frame. For θ = 45°, the maximum torque case occurs, i.e., the product sin(θcos(θ), and thus $T_{el}$ becomes maximal.

From Lenz's law, the direction of the eddy current can be predicted. The eddy current in the frame flows in a direction to oppose the field change $dB/dt$, i.e., if the magnetic field through the frame rises with time, the current in the frame flows counter to the current producing $B$ (Fig. 1), and vice versa. Consequently, the torque on the frame changes in sign. For positive $dB/dt$, the Lorentzian forces act in the directions indicated in Fig. 1 (θ = 0° is an unstable position and the frame turns to the stable position at θ = 90°). For negative $dB/dt$ the Lorentzian forces act in the opposite direction.

The frame was considered fixed at the inclination of 45° (i.e., no initial rotation was allowed, which would subsequently cause opposing voltage induction from a change of the effective area). Such an effect would stabilize the frame in its position if it had the ability to turn.

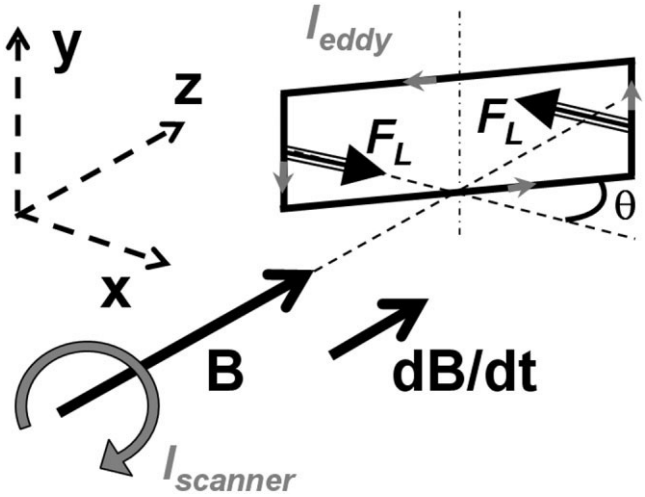


**Figure 1.** Schematic diagram for torque generation by eddy-current induction in a rectangular wire frame. Torque becomes maximal for θ = 45°, since both voltage induction and a momentum arm are necessary. The case of positive dB/dt (i.e., increasing flux through the frame) is shown. For this case, according to Lenz's law, the current in the frame flows with opposite sign compared to the current in the field-generating coil of the scanner. From the right-hand rule and the three-finger rule, it follows that the Lorentzian forces $F_L$ act as shown in the drawing.

#### *Flux Change Induced by Movement in the Fringe Field of the Scanner*

If a metallic part is moved in the inhomogenous fringe field of an MR scanner with velocity $v$ (e.g., if a patient with an implant is moved into the scanner), magnetic flux through the part changes. With a fringe-field gradient $G_{fringe}$, it holds that

$$dB/dT = v\cdot G_{fringe}. \quad (5)$$

Since the field change lasts over a relatively long period, the inductance $L$ can be neglected and the maximum achievable current is $I_{max} = U_{ind}/R$, even for a large implant.

#### *Flux Change Induced by Gradient Switching*

Another way to change the magnetic flux through a metal part is to perform gradient switching. If the part is located at a certain distance $d$ from isocenter and a gradient $G = dB/dr$ is switched, the magnetic field at this location changes for a linear gradient ramp of time τ with the rate

$$dB/dt = \Delta B/\tau = G\cdot d/\tau. \quad (6)$$

Since the magnetic field changes very fast, the maximum eddy current possible cannot be achieved during the short ramp time due to the inductance $L$ of the

metal part. The current at the end of the ramp relevant for maximum torque must be calculated from $I_{eddy}(\tau) = I_{max}(1 - e^{-\kappa\cdot\tau})$ with $I_{max} = U_{ind}/R$, and $\kappa = R/L$ as the build-up rate for the eddy current. The inductance $L$ of the conductive frame determines the time dependence of the induced current. Surprisingly, however, there is no closed-form solution for the inductance of a filamentary loop. For example, a circular loop of round wire with loop radius $r_{loop}$ and wire radius $a$ has the low-frequency inductance $L = \mu_0 \cdot r_{loop}\left[\ln\left(\frac{8r_{loop}}{a}\right) - 1.75\right]$. Since the diameter of the wire and even the exact shape of the loop have limited influence, this can be crudely approximated by $L = \mu_0 \cdot \pi \cdot r_{loop}$ (14). Although lengthy terms have been used to calculate a rectangular frame with round wire (15), an approximation using $L = \mu_0 \cdot \pi \cdot (l_1 + l_2)/2$ was proven to yield rough estimations of the interesting effects.

### *Experimental*

Both effects were examined in a 1.5 T and a 3 T scanner (Magnetom Sonata® and Magnetom Trio®; Siemens Medical Solutions, Erlangen, Germany), both of which employed active shielding. Examinations of the quadratic frames of copper and titanium, respectively, with an effective edge length of 47 mm and a conducting cross-section of $1.5 \times 3$ mm$^2$ were compared with examinations of metal plates with edge length of 50 mm and thickness of 1.5 mm made of the same materials.

Torque during movement into the scanner was measured using a special setup (Fig. 2) built in analogy to the testing apparatus described in ASTM F2213-02. The complete setup was positioned on the patient table and moved into the scanner at a constant velocity of 20 cm/second. If an electromagnetic torque was active, the specimen twisted a plastic stripe, which produced a counter torque. The initial inclination of the frame or plate was chosen to obtain an inclination of 45°. The related mechanical torque was determined by using a spring scale and measuring the force necessary at a certain lever to obtain the same roll-up.

Effects from the quickly alternating torque due to gradient switching could only be investigated qualitatively. Initially the specimens were suspended approximately 20 cm from the bore axis at half the length of the scanner tube at an inclination of 45° with respect to the main field. They were observed visually during the execution of sequences with different gradient strengths and repetitions (spatial resolution, bandwidths, as well as repetition times (TRs) and echo times (TEs) were varied in spin-echo and gradient-echo sequences). In addition to this visual method, a tactile registration of the expected vibrations was performed. The specimens were held between the thumb and index finger at different locations in the scanner tube during sequence execution. The inclination was varied. The independent observations of two persons were compared.

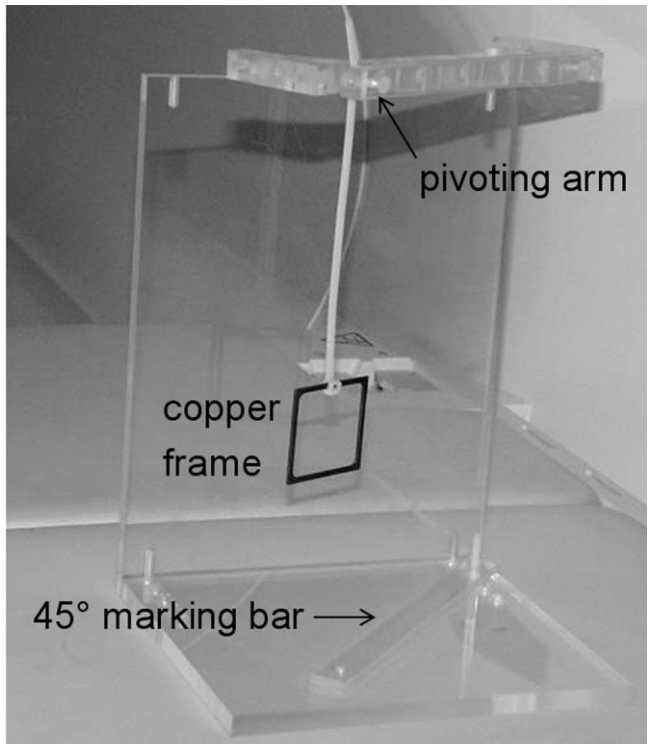


**Figure 2.** Apparatus for measuring electromagnetic torque on a copper frame at the entrance into the bore of the 3 T MR unit. The photograph was taken while the patient table was stationary. The pivoting arm was adjusted to obtain a 45° orientation of the frame (i.e., alignment parallel to the marking bar). A significant roll-up occurred during movements of the table.

## RESULTS

### *Theoretical Calculations*

For both examined sources of eddy-current induction, Eq. [4] predicts $T_{el}$ to depend on the frame parameters $A$ and $R$ with $A^2/R$. There is a linear dependence on the static field $B_0$, and maximum torque is obtained at an inclination $\theta = 45°$.

Torque caused by movement in the fringe field was calculated using Eqs. [4] and [5]. Derived torque values $T_{el}$ related to movement-induced eddy currents in metallic frames of different geometries, and the materials used are listed in Table 1. The fixed parameters were $B_0 = 1.5$ T, $v = 0.2$ m/second, $G_{fringe} = 2$ T/m, frame inclination $\theta = 45°$. Torque increased with the frame area $A$ and with the reduction of $R$. The ratio $\eta = T_{el}/T_{me}$ is independent of the cross-section $q$ of the conductor. Aluminum displays a low density at high conductivity. For a $6 \times 6$ cm$^2$ frame made of this material, the limits given in ASTM F2213-02 would be exceeded.

Torque caused by gradient switching was estimated with consideration of the inductance of the conductive frames.

Table 2 lists the torque values for the considered frames resulting from gradient switching. The fixed parameters were $B_0 = 1.5$ T, gradient amplitude $G = 40$ mT/m, distance from isocenter $d = 20$ cm, gradient ramp time $\tau = 250$ μs, and frame inclination $\theta = 45°$. Maximum torque was nearly two orders of magnitude

Table 1
Torque $T_{et}$ Induced in Wire Frames by Movement in the Fringe Field for $B_0$ = 1.5 T, v = 0.2 m/second, $G_{fringe}$ = 2 T/m, and Frame Inclination $\theta$ = 45°*

| Material | $l_l$ [cm] | $l_s$ (cm) | $q$ (mm$^2$) | Theoretical $I$(A) | Theoretical $T_{el}$(μNm) | $T_{me}$ (μNm)[a] | η | measure $T_{el}$ (μNM) |
|---|---|---|---|---|---|---|---|---|
| Cu | 2 | 0.5 | 3.14 | 0.105 | 11 | 283 | 0.04 | – |
| Cu | 4 | 1 | 3.14 | 0.209 | 89 | 1133 | 0.08 | – |
| Cu | 4.7 | 4.7 | 4.50 | 0.877 | 2055 | 4906 | 0.42 | – |
| Al | 4 | 1 | 3.14 | 0.134 | 57 | 343 | 0.17 | – |
| Al | 6 | 6 | 3.14 | 0.503 | 1921 | 1695 | 1.13 | – |
| Ti | 4 | 1 | 3.14 | 0.006 | 2.7 | 573 | 0.005 | – |
| Ti | 8 | 3 | 3.14 | 0.018 | 44 | 2611 | 0.02 | – |
| Ti | 4.7 | 4.7 | 4.50 | 0.027 | 63 | 2479 | 0.03 | – |

[a]The given mechanical torque $T_{me}$ is the maximal torque due to gravity (weight times largest dimension).
$l$, long/short side of the frame, $q$, conducting cross-section, $I$, resulting current.

higher than that for movement-induced torque. For all of the copper frames and the aluminum frame, the parameters resulted in a relatively small eddy-current build-up rate $\kappa = R/L$, i.e., the maximum current $I(\tau)$ achieved during the gradient ramp was smaller than $I_{max} = U_{ind}/R$. The poorly conducting titanium specimens allowed for a significantly faster build-up rate, with $I(\tau) \approx I_{max}$. As a result, maximum torque for the copper specimens was less than a factor of 32 higher compared to the titanium specimens of the same geometry. This factor would be expected from the ratio of the conductivities of the two materials (Table 3). Titanium is approximately half as dense as copper (Table 3). Nevertheless, for the two larger titanium specimens, the ratio $\eta$ sometimes exceeded 100% of the mechanical torque $T_{me}$. For the selected copper and aluminum frames, up to $\eta = 26$ was predicted for $B_0 = 1.5$ T.

## *Experiments*

### *Movement in the Fringe Field*

Maximum torque was found at approximately 20 cm inside the scanner bores (Fig. 2, white arrow). The manufacturer confirmed that at this point the product $B \cdot dB/dz$ becomes maximal. The experimentally determined values for the copper frame were in good agreement with the calculated values. On the 1.5 T scanner, torque was 2000 μNm ± 20% estimated systematic error due to uncertainties resulting from the force measurement with the spring scale at a certain lever arm, and additionally from the visual determination of the frame inclination during run-in of the scanner table. On the 3 T scanner, a torque of 4200 μNm ± 20% resulted. The measured torque was approximately 1.6 times larger for the copper plate than for the frame.

Compared to copper, titanium displays 32 times lower conductivity and is significantly paramagnetic (Table 3 compares these data for different materials). For the frame and the plate made of titanium, torque $T_{ma}$ resulting from the magnetization of the paramagnetic material dominated the eddy-current-induced torque. The roll-up direction was the opposite of that of the copper specimens and was largest in the homogenous static field. The torque was very small. With the accuracy of the described apparatus, it could be ascertained as being no larger than 50 μNm at 1.5 T and 100 μNm at 3 T for the frame. For the plate, no difference could be assessed with the applied method.

### *Gradient Switching Effects*

For all specimens examined, no visible rotation was seen when they were suspended near the scanner wall at an inclination $\theta = 45°$ during a sequence that exploited the gradient capabilities. However, if the specimens were held manually between the thumb and index finger, significant vibrations were reported by both observers for all samples, depending on the gradient strength and inclination in scale. The effects were clearly more pronounced at 3 T than at 1.5 T. No differences could be detected by the described method between titanium and copper or between frame and

Table 2
Torque $T_{el}$ Induced in Wire Frames by Gradient Switching at $B_0$ = 1.5 T, Gradient Amplitude $G$ = 40 mT/m, Distance from Isocenter $d$ = 20 cm, Ramp Time $\tau$ = 250 μsec, and Frame Inclination $\theta$ = 45°*

| Material | $l_l$ (cm) | $l_s$ (cm) | $q$ (mm$^2$) | κ (1/second) | $I(\tau)$ (A) | $T_{el}$ (μNm) | $T_{me}$ (μNm) | η |
|---|---|---|---|---|---|---|---|---|
| Cu | 2 | 0.5 | 3.14 | 8620 | 7.39 | 784 | 283 | 2.77 |
| Cu | 4 | 1 | 3.14 | 8620 | 14.8 | 6270 | 1133 | 5.53 |
| Cu | 4.7 | 4.7 | 4.50 | 6030 | 54.6 | 128000 | 4906 | 26.09 |
| Al | 4 | 1 | 3.14 | 13400 | 10.4 | 4390 | 343 | 12.81 |
| Ti | 4 | 1 | 3.14 | 281000 | 0.51 | 216 | 573 | 0.38 |
| Ti | 8 | 3 | 3.14 | 281000 | 1.40 | 3560 | 2611 | 1.36 |
| Ti | 4.7 | 4.7 | 4.50 | 197000 | 2.15 | 5040 | 2479 | 2.04 |

*Clearly perceptible mechanical vibrations could be verified by the described tactile method for all samples, but no quantitative experimental torque values are available.
$l_l$, $l_s$, long/short side of the frame, $q$, conducting cross-section, $I(\tau)$, current at end of ramp.

Table 3
Specific Resistance ρ, Magnetic Susceptibility $\chi_{SI}$, and Specific Weight *w* of Different Metals and Alloys Used for Medical Equipment and Implants*

| Material | ρ ($\Omega mm^2/m$) | $\chi_{SI}$ | *w* ($g/cm^3$) |
|---|---|---|---|
| Cu | 0.017 | –9.63 | 8.920 |
| Titan | 0.554 | +181.1 | 4.507 |
| Ti-6Al-4V | 1.7 | +194.9 | 4.420 |
| NiTi | 0.82 | +202.63 | 6.450 |
| Al | 0.0265 | +20.75 | 2.700 |
| CoCrNi (Eligiloy/phynox) | 0.996 | +399.8 | 8.300 |

*Sources: Handbook of Chemistry and Physics; for alloys: Matweb on line.

plate. The vibrations vanished toward isocenter. Vibrations could also be detected for positions approximately 30–40 cm off center in the z-direction.

## DISCUSSION

Eddy currents induced in metallic instruments and implants can result from a movement in the fringe field of the MR scanner or from gradient switching. In principle, the Lorentz forces that occur in strong magnetic fields are responsible for generating torque. The safety standard ASTM F 2213-02 advises limits for torque resulting from the alignment of magnetizable material to a static magnetic field. The maximum torque has to be less than the maximum torque case due to gravity being given by the product of the longest dimension and weight. Similar torque effects from eddy-current induction are not considered at the present stage. In this work we theoretically and experimentally examined conditions under which eddy-current induction could cause hazardous situations comparable to those resulting from magnetic alignment. The origin of the torque has no relevance with respect to mitigating the danger posed by counter forces, and the same limits should apply. As simple models, frame-like structures were examined. A generalization to an arbitrary geometry can be performed in accordance with a previously described approach for assessing torque from magnetizable material (2). To account for the complicated dependencies, empirical form factors were introduced.

Movement in the fringe field was found to cause only small torque under standard conditions, especially for small parts made of materials with lower conductivity. However, there are several issues that could increase the relevance of this effect. First, there is the increase of the static field strength. Second, steeper fringe field gradients of magnets with extreme active shielding will result in high *dB/dz*. Finally, future applications, which intend the patient to be moved more rapidly through the scanner, could be critical since the reported torque forces are increasing with velocity. Depending on the material of the implants and instruments used, as well as the geometrical conditions, significant effects might result.

For gradient switching, the maximum torque values were up to two orders of magnitude higher than the values resulting from movement in the fringe field under clinical standard conditions. In principle, the maximum torque can be higher than the maximum torque due to gravity (which was stated in safety standard ASTM F 2213-02 as the critical limit), but the torque lasts for only a very short time during the gradient ramps. As switching-off of a gradient induces an eddy current in the opposite direction as switching-on fast alternating torque results. No visible rotation occurs due to mass inertia, but vibration becomes clearly apparent. If, for example, an implant is located near a very sensitive area in a patient, it is very likely that unpleasant sensations will result. Complaints from patients with metallic implants during routine clinical examinations have been reported, and were explained as originating from gradient switching induced vibrations (16).

Titanium exhibits a relatively fast current rise, whereas in copper the higher current is reached more slowly. This may explain the small differences found between copper and titanium. The small difference between the plate and frame may result from an eddy-current development mainly near the edges of the plates for the fast-changing magnetic flux. Since all components of the gradient field are relevant for electromagnetic induction, metallic parts located off center in the z-direction (i.e., relatively far away from the patient region under investigation) can be affected.

Initial tests were carried out at 1.5 T on various implants (stents, aneurysm clips, refixation implants for cranial bone flaps after craniotomy, artificial vertebral disks, and artificial hips). If they were made of a poorly-conducting metal (i.e., titanium, nitinol, or TiAl4V6), the size of the implant must be larger than approximately 10 centimeters to slightly sense vibrations at high gradient amplitudes. Strong vibration occurred in an artificial hip replica made of aluminum, which in principle should have better MR compatibility due to smaller susceptibility artifacts (Table 3). Frame-like metallic vertebral column stabilization (comparable to the examined titanium frame) offers a highly conductive cross section for eddy currents. Since it is located near the spinal cord, a high potential for undesired nerve irritation must be assumed.

To conclude, we have demonstrated that torque acting on metallic implants or instruments due to eddy-current induction can be considerable and exceed the current limits for torque resulting from the alignment of magnetizable material. It should be noted that larger parts made from well-conducting materials are especially affected. Torque due to movement in the fringe field could gain in importance in future applications with high-field scanners, and if patient table velocity is increased. Gradient switching was shown to produce fast alternating torque. Significant vibrations at off-center positions of the metal parts may explain why patients with an extended metallic implant sometimes report feeling sensations during MR examinations.

Consideration should therefore be made to extend safety testing of extended implants or instruments with respect to the described mechanisms, especially if they are made of well-conducting materials. Material with low susceptibility and with low conductivity is required to achieve MR-safety in medical implants and instruments. Special geometrical constructions of the devices

that generate high electrical resistance for eddy currents may represent an alternate solution for these problems.

## ACKNOWLEDGMENT

The authors thank Jane Gollub for revising the language of the manuscript.

## REFERENCES

1. Specific standard of the "American Society for Testing and Materials" ASTM F 2213-02: measurement of magnetically induced torque on passive implants in the magnetic resonance environment.
2. Schenck JF. Safety of strong, static magnetic fields. J Magn Reson Imaging 2000;12:2–19.
3. Teissl C, Kremser C, Hochmair ES, Hochmair-Desoyer IJ. Magnetic resonance imaging and cochlear implants: compatibility and safety aspects. J Magn Reson Imaging 1999;9:26–38.
4. Teissl C, Kremser C, Hochmair ES, Hochmair-Desoyer IJ. Cochlear implants: in vitro investigation of electromagnetic interference at MR imaging—compatibility and safety aspects. Radiology 1998; 208:700–708.
5. Shellock FG. Metallic neurosurgical implants: evaluation of magnetic field interactions, heating, and artifacts at 1.5-Tesla. J Magn Reson Imaging 2001;14:295–299.
6. Shellock FG. Metallic surgical instruments for interventional MRI procedures: evaluation of MR safety. J Magn Reson Imaging 2001; 13:152–157.
7. Edwards MB, Taylor KM, Shellock FG. Prosthetic heart valves: evaluation of magnetic field interactions, heating, and artifacts at 1.5 T. J Magn Reson Imaging 2000;12:363–369.
8. Schueler BA, Parrish TB, Lin JC, et al. MRI compatibility and visibility assessment of implantable medical devices. J Magn Reson Imaging 1999;9:596–603.
9. Shellock FG. Biomedical implants and devices: assessment of magnetic field interactions with a 3.0-Tesla MR system. J Magn Reson Imaging 2002;16:721–732.
10. Shellock FG, Hatfield M, Simon BJ, et al. Implantable spinal fusion stimulator: assessment of MR safety and artifacts. J Magn Reson Imaging 2000;12:214–223.
11. Sullivan PK, Smith JF, Rozzelle AA. Cranio-orbital reconstruction: safety and image quality of metallic implants on CT and MRI scanning. Plast Reconstr Surg 1994;94:589–596.
12. Shafiei F, Honda E, Takahashi H, Sasaki T. Artifacts from dental casting alloys in magnetic resonance imaging. J Dent Res 2003;82: 602–606.
13. Robertson NM, Diaz-Gomez M, Condon B. Estimation of torque on mechanical heart valves due to magnetic resonance imaging including an estimation of the significance of the Lenz effect using a computational model. Phys Med Biol 2000;45:3793–3807.
14. Wheeler HA. Formulas for the skin effect. In: Proceedings of the 30th Annual Meeting of IRE, 1942. p 412–424.
15. Grover W. Inductance calculations: working formulas and tables. New York: Dover Publications, Inc.; 1946.
16. Hartwell RC, Shellock FG. MRI of cervical fixation devices: sensation of heating caused by vibration of metallic components. J Magn Reson Imaging 1997;7:771–772.